Towards Noninvasive Assessment of Arterial Stiffness: Regression Modeling from Radial-Tibial Pulse Wave Features

Marco Pogliano, *Member, IEEE*, Alessandro Sanginario, *Member, IEEE*, Irene Buraioli, *Member, IEEE*, Dario Leone, Alberto Milan and Danilo Demarchi, *Senior Member, IEEE*

***Abstract*— In the last decade, research in developing systems for monitoring clinical parameters has grown exponentially, driven by the increasing demand for continuous and remote observation. Monitoring cardiovascular diseases (CVD) is crucial, as they remain the leading cause of mortality worldwide. Pulse Wave Velocity (PWV) is a key clinical indicator for assessing arterial stiffness, highly correlated with CVD. Current methods for measuring PWV require acquiring pulse wave signals at the carotid and femoral sites, configurations that are widely validated in the literature. However, accessing these specific anatomical points presents a significant challenge for developing wearable devices for continuous or home-based PWV monitoring. The present study proposes an innovative approach using a regression algorithm to predict the carotid-femoral PWV value from pulse waves acquired at more accessible sites, including the carotid, radial, and tibial, compatible with wearable use. The study was conducted on a cohort of 90 voluntary healthy participants at the Candiolo Cancer Institute FPO-IRCCS. The best-performing carotid-radial models show a mean error (ME) of less than 0.1 m/s, with a standard deviation error (SDE) below 1 m/s. Similarly, the radial-tibial models exhibit a mean error of the same magnitude but with an even smaller standard deviation error, below 0.9 m/s. These results highlight the strong predictive capabilities of the developed models, offering promising prospects for future clinical implementation aimed at noninvasive and potentially continuous vascular health monitoring.**

***Index Terms*— Arterial Stiffness, Cardiovascular Diseases (CVDs), Pulse Wave Velocity (PWV), Radial-Tibial PWV, Regression Modeling**

I. Introduction

ATHEROSCLEROSIS is the primary underlying cause of cardiovascular diseases (CVD), which continue to be the leading cause of global mortality [1], [2]. This pathological condition, defined as the accumulation of lipids, inflammatory cells, and fibrous elements on the arterial wall, significantly alters normal blood flow. The reduction in vessel lumen can lead to acute occlusions, resulting in thrombus formation and critical events such as myocardial infarction and stroke [3]. Cardiovascular diseases, closely related to hypertension, can be monitored through arterial stiffness assessment, a key indicator for evaluating the functional status of the cardiovascular system. Increased stiffness of the arterial walls impairs the vessels' ability to adequately modulate blood flow, generating hemodynamic overload on the heart and eventually leading to ventricular hypertrophy [4]–[6]. In this context, Pulse Wave Velocity (PWV) is increasingly recognized as a reference parameter, not only in scientific research but also in clinical practice, as it provides a non-invasive estimate of arterial stiffness. Recent studies have linked increased arterial stiffness to greater cognitive decline in elders [7], and scientific evidence consistently demonstrates that elevated vascular stiffness is associated with a higher PWV, reflecting accelerated pulse wave propagation along the arterial tree [8], [9].

PWV is calculated as the ratio between the physical distance between two arterial sites and the time delay of pulse wave propagation between them. The most commonly used reference sites in the literature are the carotid and femoral sites, which have shown a high correlation with arterial stiffness and significant predictive value [10]. Several algorithms have been proposed to estimate the time offset between signals, including intersecting tangent point [11], cross-correlation [12], and second derivative methods [11], with the intersecting tangent point being the most widely used in clinical devices due to its robustness under varying operational conditions. The choice of acquisition methodology and processing algorithm directly impacts the usability of the device and the ease of using PWV as a clinical parameter. Advances in transduction technologies have significantly expanded the options for pulse wave detection [13]. Common solutions currently include applanation tonometers (SphygmoCor Vx [14], [15], SphygmoCor XCEL [16], [17], PulsePen [18], Athos [19], [20]), oscillometry using cuffs (e.g., Vicorder [21], Arteriograph [22]), mechanical piezoelectric transducers (Complior [23]), and photoplethysmography (MPPT [24]). A comparative summary of these devices is provided in Table I, referencing the type of sensor and the execution mode. Acquisition methodologies are generally divided into two main categories: two-step and one-step. In the two-step mode, Figure 1a, the ECG signal

Marco Pogliano, Alessandro Sanginario, Irene Buraioli and Danilo Demarchi are with the Department of Electronics and Telecommunications, Politecnico di Torino, 10129 Torino, Italy (e-mail: marco.pogliano@polito.it; alessandro.sanginario@polito.it; irene.buraioli@polito.it; danilo.demarchi@polito.it).

Dario Leone and Alberto Milan are with the Candiolo Cancer Institute FPO-IRCCS, Division of Internal Medicine, Department of Medical Science - University of Turin, 10060 Candiolo (TO), Italy (e-mail: dario.leone@ircc.it; alberto.milan@ircc.it).

is recorded simultaneously with the pulse wave at one site, followed by acquisition at the second site. The R-wave of the QRS complex serves as a common time reference for realigning the two signals acquired at different times. In the one-step mode pulse waves are simultaneously acquired at both sites, without the need for an external ECG reference signal (Figure 1b). One of the factors that most significantly impacts the reliability of PWV measurements is the level of clinical experience of the operator [25]. This is particularly relevant for identifying the two commonly used measurement sites, especially the femoral site, which is notoriously complex and challenging to locate accurately. This difficulty in sensor placement at the femoral site also poses a significant barrier to developing wearable devices for remote and continuous PWV monitoring.

The primary objective of this study is to develop a predictive model capable of estimating carotid-femoral Pulse Wave Velocity (cf-PWV) through the use of alternative peripheral acquisition sites. The selection of candidate sites was carried out in close collaboration with the medical team, an integral part of the research group, with the aim of identifying anatomical locations that ensure both improved accessibility and high signal reliability. Specifically, the radial and tibial arteries, the latter representing a novel contribution of this study, were identified as ideal candidates, as they facilitate artery localization, simplify acquisition procedures, reduce operational time, and enable the test to be performed by non-specialist personnel. Two innovative scenarios were considered: (1) the carotid–radial combination and (2) the radial–tibial combination, as illustrated in Figure 1c. The latter configuration was examined in greater detail due to its potential integration into wearable systems, for instance through the use of a wristband and an ankle strap—solutions that would be considerably less feasible using the traditional carotid and femoral sites. Furthermore, the robustness of the developed models was enhanced by incorporating physiological parameters, such as heart rate, blood pressure, weight, and height, which significantly influence PWV measurement, as discussed in [8], into the model training.

Device	Sensor	Execution Mode
SphygmoCor Vx	Tonometric	Two step
Pulse Pen	Tonometric	Two step
SphygmoCor XCEL	Tonometric	One step
Athos	Tonometric	One step
Vicorder	Cuff-based oscillometry	One step
Arteriograph	Cuff-based oscillometry	One step
Complior	Piezoelectric	One step
MPPT	PPG	One step

TABLE I: The main research and commercial devices for Pulse Wave Velocity assessment.

The document is organized as follows: Chapter II describes the data acquisition protocol, signal processing techniques, regression models used, and validation methodologies employed; Chapter III analyzes the main clinical recommendations related to PWV prediction and presents the results obtained for both datasets; Chapter IV discusses the results in the context of existing literature, highlighting strengths and challenges; Chapter V presents the conclusions and future perspectives.

II. Methods

This section provides a detailed description of the pulse wave signal acquisition protocol employed by the medical staff, along with the techniques used for data pre-processing

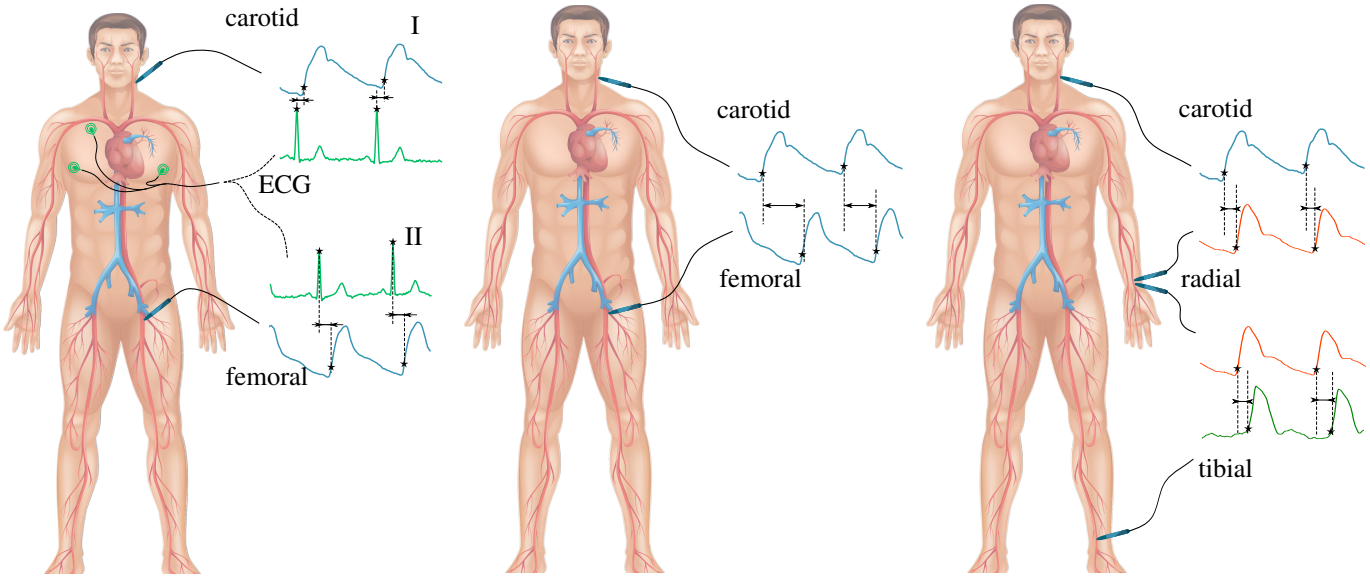

(a) cf - two step mode (b) cf - one step mode (c) innovative approach

Fig. 1: (a) Carotid-femoral (cf) two step mode; (b) Carotid-femoral (cf) one step mode; (c) Innovative approach using carotid-radial-tibial acquisition sites.

and the identification of potential outliers. Subsequently, the regression models considered are analyzed, and the validation metrics adopted for assessing predictive performance are discussed.

A. Data

This study was designed to develop a predictive model for the cf-PWV value by analyzing pulse wave signals acquired at peripheral sites in a cohort of 90 healthy subjects. Participants were recruited through targeted cardiovascular health outreach at hospitals, supported by professional networks. Inclusion criteria required participants with no prior history of cardiovascular disease or conditions that could influence arterial stiffness. The exclusion criteria comprised a Body Mass Index (BMI)$> 40\,\mathrm{kg/m^2}$, age < 18 or > 80 years, subject with a history of stroke, diabetes, or hypertension, as well as those who were pregnant or had any significant medical conditions that could alter the cardiovascular system. Data acquisition was performed by experienced medical professionals at the Candiolo Cancer Institute FPO-IRCCS, Division of Internal Medicine, Department of Medical Sciences, with ethical approval granted by the Bioethics Committee of the University of Turin (Protocol No. 161272, March 8, 2021). All participants provided informed consent before enrollment. The data used in this study were acquired using the SphygmoCor system, a clinically validated device, in order to ensure the development of a reliable and robust dataset. This choice was motivated by the need to obtain high-quality signals while minimizing potential biases introduced by experimental instrumentation. Pulse waves were recorded at four anatomical sites: carotid, femoral, radial, and tibial. For each of the two pairs of interest, carotid-femoral and radial-tibial, a clinical report was generated, which included all relevant parameters for the examination, such as medical history, blood pressure, cardiac parameters, Pulse Transit Time (PTT), and PWV. These reports formed the dataset on which the present study is based. In the initial phase of the study, a systematic extraction of all parameters from the reports for each acquisition was conducted. For each volunteer subject, three measurements were taken for each site pair. The acquisition protocol was designed to minimize operator-induced bias, as the literature highlights the significant impact of the operator's clinical experience on data quality [25]. To mitigate this bias, as shown in Figure 2, acquisitions were performed by alternating operators between consecutive subjects for each measurement device. The demographic characteristics of the study population (gender, age, height, and weight) ensure a high degree of heterogeneity within the sample, in accordance with the criteria outlined in [26]. The sample exhibits an excellent gender balance (46 females, 44 males), an appropriate distribution of body weight ($69.7 \pm 13.6\,\mathrm{kg}$), a well-represented age stratification (<30 years: 18 subjects; 30–49 years: 11 subjects; 50–69 years: 51 subjects; ≥70 years: 10 subjects), and a suitable distribution of cf-PWV values ($\leq 6\,\mathrm{m/s}$: 16 % of subjects; $\geq 8\,\mathrm{m/s}$: 42 % of subjects; $\geq 10\,\mathrm{m/s}$: 11 % of subjects).

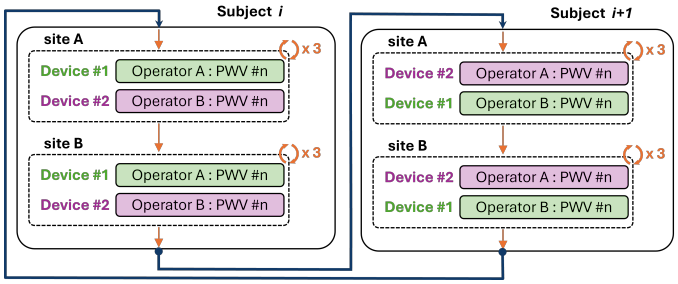

Fig. 2: The figure illustrates the protocol adopted for data acquisition, which involves the systematic alternation of operators to minimize bias associated with their skills and clinical experience.

B. Pre-processing

For each clinical report generated, the following parameters were extracted: age, gender, height, weight, distance between the measurement sites, systolic pressure, diastolic pressure, PTT for each site (A and B), including mean and standard deviation values, PTT differential (mean and standard deviation), heart rate, and the mean PWV value with the corresponding standard deviation. For each subject, the extracted data were organized and associated with the four considered measurement sites (carotid, femoral, radial, and tibial) to construct a set of features for each site. Parameters associated with multiple sites were duplicated to ensure the internal consistency of the dataset. The data were averaged for each trial of acquisitions related to the same subject and site to obtain a single feature array representative of the subject. The average was calculated only on data deemed of adequate quality. This assessment was conducted under medical supervision, focusing on the cf-PWV values. If any value within the triad deviated by more than 15% from the median value, the entire acquisition was excluded from the analysis as it was considered unreliable.

At the end of this phase, two distinct datasets were constructed, each intended to develop a different regression model. The first dataset includes all unique vectors related to the carotid and radial sites, while the second contains features associated with the radial and tibial sites.

C. Regression Models

The construction of the predictive model for the two datasets tested the performance of various regressors from different classes, thus avoiding any prior assumptions about the relationships between the variables and the output. Specifically, the regressors from the following classes were studied.

1) Linear Regression and Generalizations: These models are based on a linear relationship between input and output, being simple and interpretable. Linear regression is the basic model. Ridge, Lasso, and ElasticNet Regression add regularization (L2, L1, or both). Bayesian Ridge and Automatic Relevance Determination (ARD) Regression introduce a Bayesian perspective. The Poisson Regressor, and Tweedie Regressor extend linear regression to non-Gaussian targets. Quantile Regressor estimates quantiles instead of the mean.

The Transformed Target Regressor allows for target transformations during training.

2) Robust Regression and Noisy Data: These models suit data with outliers or anomalies. Huber Regressor combines Mean Squared Error (MSE) and Mean Absolute Error (MAE) for greater robustness. The Theil-Sen Regressor is highly resistant to outliers but slower. Random Sample Consensus Regressor builds models on subsets, ignoring inconsistent points. Stochastic Gradient Descend (SGD) Regressor uses stochastic gradient descent.

3) Nonlinear Kernel-Based Regression: These models utilize kernels to model complex relationships, as Support Vector Regressor (SVR) and NuSVR.

4) Tree-Based and Ensemble Regression: These flexible models are based on decision trees, often combined to improve stability. Decision Tree is the base model. Random Forest and Extra Trees enhance generalization and speed. Gradient Boosting and Histogram Gradient Boosting build trees sequentially. AdaBoost weights complex examples, Bagging uses models on subsamples.

5) Regression Based on Neighbors and Monotonicity: These models rely on the proximity of observations or monotonicity constraints. K-Nearest Neighbors Regressor and Radius Neighbors Regressor predict based on nearby points. Polynomial Regression, obtained through polynomial transformations, captures nonlinearity while maintaining good interpretability.

D. Validation techniques

For the training and validation of the developed models, the original dataset was split into two subsets: a training set (80%) and a test set (20%). In this way, the data from the test set, which were not accessible during the learning phase, were used to evaluate the models' accuracy and robustness in predicting unseen data. The split was carried out stochastically, but an initial seed was selected to ensure maximum similarity between the distributions of cf-PWV values in the two subsets. This approach was adopted to ensure that both sets representatively covered the entire spectrum of PWV values in the dataset. Although this condition is generally met with a sufficiently large dataset, it must be carefully verified in contexts characterized by a limited number of observations. The performance evaluation of the models was conducted using two standard metrics: Mean Error (ME) and Standard Deviation Error (SDE). These metrics are essential tools for quantifying the quality of a regression model, as they measure the degree of deviation between the predicted values and the actual observed values. Each of the presented algorithms was trained, where applicable, using various optimization metrics. Among these, the metrics that proved to be the most robust and led to the best results were the coefficient of determination (R^2), mean absolute error (MAE), mean squared error (MSE), and mean absolute percentage error (MAPE).

III. Results

A. PWV Recommendation

Given the highly specialized nature of the medical-clinical context in which this research is embedded, validating a new device or algorithm must adhere to rigorous and well-defined criteria. In the case of PWV, new official recommendations were published in 2024 [26], providing specific guidelines for

Methods	Carotid-Radial					Radial-Tibial				
	Training metric	ME (m/s)	SDE (m/s)	MAE (m/s)	MSE $(m/s)^2$	Training metric	ME (m/s)	SDE (m/s)	MAE (m/s)	MSE $(m/s)^2$
ARD Regression	R^2	**0.139**	**0.904**	0.744	0.791	R^2	-0.068	0.930	0.686	0.821
AdaBoost Regressor	MAE	-0.123	1.062	0.837	1.081	R^2	-0.113	0.976	0.740	0.913
Bagging Regressor	MSE	-0.132	1.118	0.865	1.197	MAE	-0.128	0.950	0.664	0.870
Bayesian Ridge Regression	R^2	0.088	0.984	0.817	0.922	MAE	-0.091	1.007	0.777	0.965
Decision Tree Regressor	MAE	-0.253	1.256	0.998	1.554	R^2	0.061	1.258	0.949	1.498
ElasticNet Regression	R^2	0.006	1.372	1.107	1.777	R^2	-0.011	1.362	1.099	1.752
Extra Trees Regressor	MAE	0.071	1.050	0.823	1.047	MSE	-0.041	0.957	0.698	0.866
Gradient Boosting Regressor	R^2	-0.152	1.054	0.765	1.072	R^2	-0.103	0.981	0.712	0.920
Histogram Gradient Boosting Regressor	R^2	**-0.145**	**0.830**	0.706	0.671	R^2	-0.207	1.003	0.798	0.992
Huber Regressor	MAE	**0.143**	**0.911**	0.722	0.804	MAE	**0.098**	**0.851**	0.696	0.693
K-Nearest Neighbors Regressor	R^2	0.354	1.387	1.114	1.941	R^2	-0.120	1.511	1.201	2.171
Lasso Regression	R^2	0.054	1.109	0.872	1.164	R^2	-0.010	1.116	0.859	1.175
Linear Regression	R^2	0.142	0.914	0.728	0.809	R^2	0.187	0.889	0.725	0.782
Nu Support Vector Regressor (nuSVR)	MAPE	0.286	1.329	1.069	1.751	R^2	-0.185	1.312	1.027	1.660
Poisson Regressor	MAE	**0.154**	**0.813**	0.657	0.649	R^2	**-0.036**	**0.903**	0.709	0.771
Polynomial Regression	MAPE	0.275	1.793	1.370	3.112	R^2	0.658	1.420	1.199	2.336
Quantile Regressor	MAE	-0.333	1.573	1.263	2.448	MAE	-0.333	1.573	1.263	2.448
Random Sample Consensus Regressor	R^2	0.242	1.087	0.855	1.175	R^2	-0.382	1.221	1.006	1.554
Radius Neighbors Regressor	R^2	-0.041	1.562	1.261	2.307	R^2	-0.026	1.536	1.247	2.229
Random Forest Regressor	MAE	-0.114	1.088	0.880	1.131	MAE	-0.121	1.019	0.710	0.995
Ridge Regression	R^2	0.053	1.052	0.854	1.047	MAE	**0.015**	**0.882**	0.668	0.735
Stochastic Gradient Descend (SGD) Regressor	R^2	-0.008	1.382	1.157	1.803	MSE	-0.079	1.363	1.124	1.761
Support Vector Regressor (SVR)	MAPE	0.382	1.212	1.068	1.534	R^2	-0.087	1.315	1.034	1.641
Theil-Sen Regressor	MAE	0.123	0.956	0.798	0.879	R^2	**0.134**	**0.851**	0.705	0.702
Transformed Target Regressor	R^2	0.142	0.914	0.728	0.809	R^2	0.187	0.889	0.725	0.782
Tweedie Regressor	MAE	**0.154**	**0.813**	0.657	0.649	R^2	**-0.036**	**0.903**	0.709	0.711

TABLE II: Best results on the Test Set for each classifier were analyzed as Mean Error (ME), Standard Deviation of the Error (SDE), Mean Absolute Error (MAE), Mean Squared Error (MSE) for both the Carotid-Radial and Radial-Tibial datasets.

both the composition of the study sample and the minimum performance requirements for predictive models. Regarding the experimental population, the guidelines suggest including no fewer than 85 subjects evenly distributed across different age groups and between the two genders. It is also recommended that PWV values be equally represented across the entire physiological spectrum to ensure the generalizability of the results. Additionally, certain exclusion criteria are outlined, such as being under the legal age of adulthood and having a Body Mass Index (BMI) exceeding a predetermined threshold. The guidelines also introduce uncertainty bands that ensure at least 85% of the predictions fall within clinically acceptable error limits. Specifically, they define a clear inverse relationship between the mean error and the corresponding maximum allowable standard deviation of the error, in order to guarantee the accuracy of the measurements. In particular, for a mean error below $0.2\,\mathrm{m/s}$, which is considered acceptable by the clinical team, the standard deviation of the error must be lower than $0.664\,\mathrm{m/s}$ to ensure high accuracy, or below $1.022\,\mathrm{m/s}$ to be considered within acceptable accuracy. These thresholds were adopted as reference criteria for the final validation of the developed models, although they were originally established for the validation of new physical measurement devices and not for algorithms based on machine learning techniques. For this specific purpose, which includes the present study, it is clearly stated that no official, consolidated guidelines currently exist; therefore, these recommendations were used as a reference point, while acknowledging the difference in their intended application. It is also important to note that the threshold values provided refer to a validation population consisting of at least 85 subjects, a sample size that is difficult to achieve in our case through a simple 80/20 split of the available dataset. To overcome this limitation and ensure a more comprehensive validation, we carried out an additional analysis phase using Leave-One-Out (LOO) validation, applied to the models that demonstrated the best performance in the initial study phase. This approach involved retraining the model for each subject, each time using the entire dataset minus one instance for training and reserving the excluded subject as an independent test set. In this way, each sample was used exactly once as an unseen instance for the algorithm, as done in [27]. While we acknowledge that this approach does not provide the same level of statistical robustness as the traditional training/validation split, it nonetheless allows the application of the clinical guideline metrics for an objective assessment of model quality. As a result, this strategy enabled a deeper investigation into the feasibility of employing machine learning–based predictive techniques and data acquired from

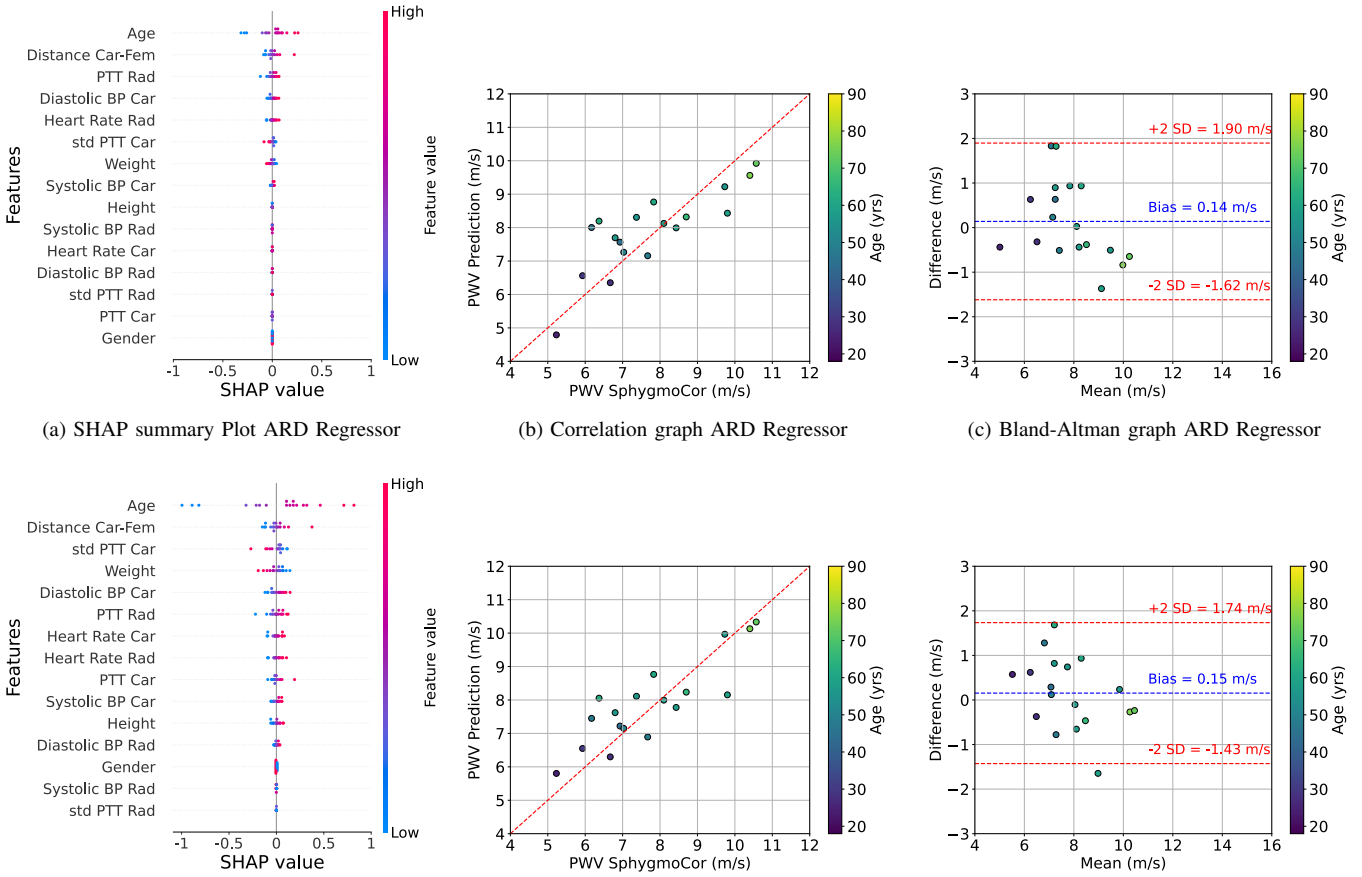

(a) SHAP summary Plot ARD Regressor (b) Correlation graph ARD Regressor (c) Bland-Altman graph ARD Regressor

(d) SHAP summary Plot Poisson Regressor (e) Correlation graph Poisson Regressor (f) Bland-Altman graph Poisson Regressor

Fig. 3: SHAP summary plot, correlation graph, Bland-Altman plot for the Carotid-Radial Test Set for the ARD Regression model (a-b-c) and the Poisson Regression model (d-e-f).

alternative measurement sites for the estimation of cf-PWV. In clinical practice, a threshold of 9 m/s is commonly used to discriminate between subjects who may exhibit symptoms and, consequently, require further diagnostic investigations. The impact of predictive error on the correct clinical classification of subjects was therefore used as a second discriminating factor in the comparative analysis of the models.

B. Carotid-Radial

The results obtained from all the regression algorithms trained on the Carotid-Radial data are presented in Table II. For each model the ME and SDE, calculated on the Test Set (comprising data never used during training), are reported to assess the models' ability to generalize on unseen data. It is observed that some configurations, such as Polynomial Regression, Quantile Regressor, and Radius Neighbors Regressor, perform worse. This behavior was attributed to a slight overfitting phenomenon relative to the training data, resulting in a reduced generalization ability. The best models on this specific dataset were ARD Regression, Histogram Gradient Boosting, Huber Regressor, Poisson Regressor, and Tweedie Regressor. These models exhibit comparable ME and SDE results, suggesting robust and consistent behavior. Therefore, the selection of the two optimal models was guided by the analysis of the error distribution related to MAE and MSE, and the impact that the predictive error might have on the potential misclassification of a subject as "potentially symptomatic". For the two selected best models, Poisson Regressor and ARD Regressor, their respective SHAP summary plots, correlation graphs between predicted and actual values, as well as Bland-Altman analyses, are presented in Figure 3. The SHAP summary plots (Figure 3a-3d) highlight that age, the carotid-femoral distance, radial PTT, and carotid PTT variability are among the most influential variables for both models. The well-known positive correlation between age and PWV is also confirmed: younger age tends to lower the estimated PWV value while older age increases. In contrast, variables such as radial blood pressure, gender, and height have negligible contributions to the prediction. The correlation graphs (Figure 3b-3e) reveal a strong agreement between predicted and observed values, with both models correctly distinguishing "potentially symptomatic" subjects, except for a single case. This high accuracy is also reflected in the Bland-Altman analysis (Figure 3c-3f), where a clear tendency toward error flattening around

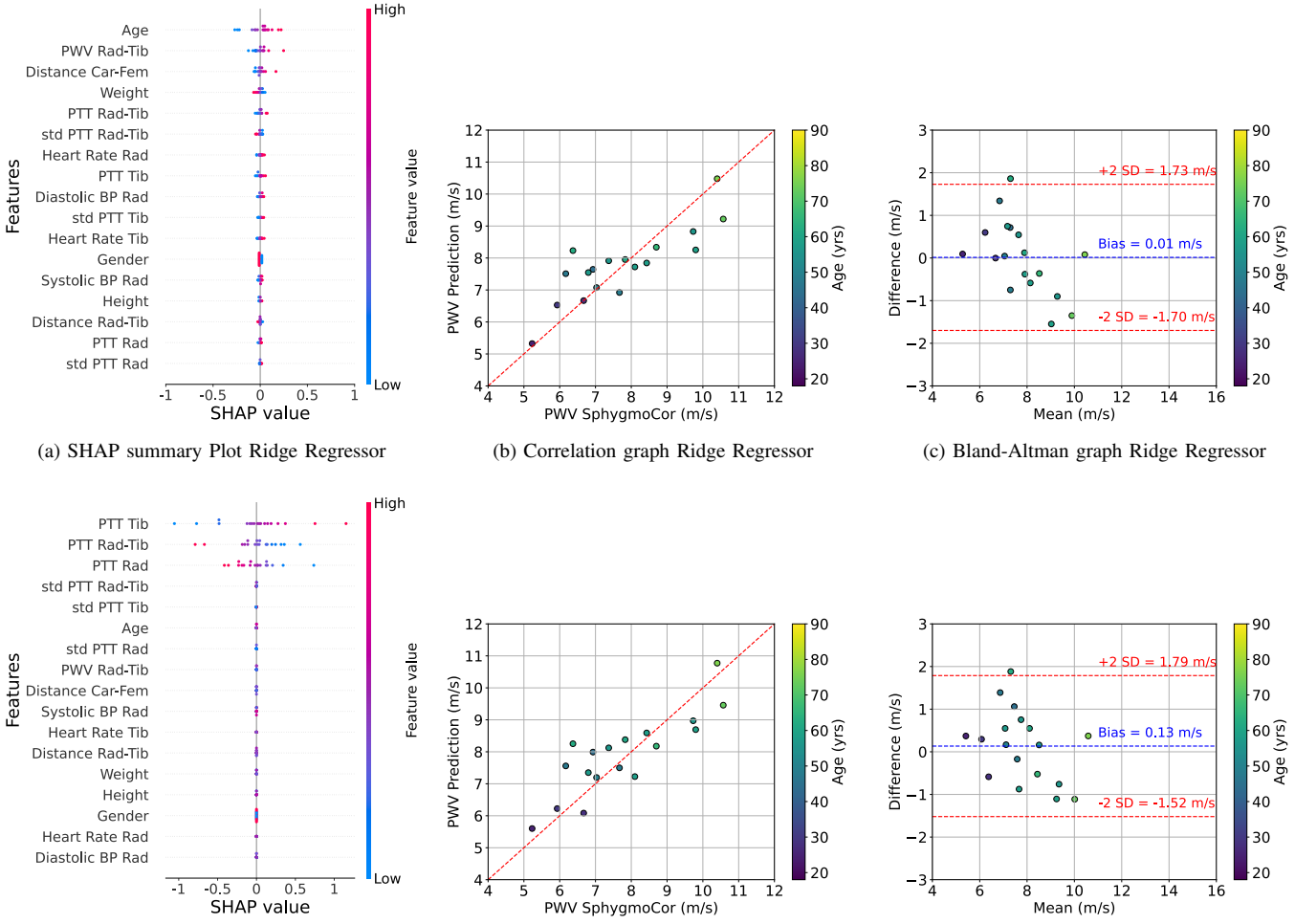

(a) SHAP summary Plot Ridge Regressor (b) Correlation graph Ridge Regressor (c) Bland-Altman graph Ridge Regressor

(d) SHAP summary Plot Theil-Sen Regressor (e) Correlation graph Theil-Sen Regressor (f) Bland-Altman graph Theil-Sen Regressor

Fig. 4: SHAP summary plot, correlation graph, Bland-Altman plot for the Radial-Tibial Test Set for the Ridge model (a-b-c) and the Theil-Sen Regressor model (d-e-f).

zero is observed. The two models identified as the most effective in modelling the phenomenon under investigation were subjected to an additional validation using the Leave-One-Out (LOO) approach, iteratively applied to all 90 entries in the dataset, each of which was used once as an unseen instance during training. The results indicate that the ARD Regression model yielded a mean error of $0.007\,\mathrm{m/s}$ with a standard deviation of $1.022\,\mathrm{m/s}$; the Poisson Regressor model achieved a mean error of $0.006\,\mathrm{m/s}$, with a standard deviation of $0.962\,\mathrm{m/s}$. Consistent with the recommendations previously discussed, the observed bias and standard deviation values support the potential reliability of both selected models, with the Poisson Regressor exhibiting overall superior performance.

C. Radial-Tibial

Regarding the Radial-Tibial dataset, the results from the regression models training are also presented in Table II. A preliminary comparative analysis reveals that the performance of most models is essentially equivalent to that achieved on the Carotid-Radial dataset, suggesting that the use of the carotid site is not strictly necessary for predictive purposes. The five models that showed the best performance on this dataset were Huber Regressor, Poisson Regressor, Ridge Regressor, Theil-Sen Regressor, and Tweedie Regressor. Some of these overlap with those previously identified as optimal for the Carotid-Radial dataset, confirming their effectiveness in accurately modeling the phenomenon under study. Similarly, the least performing models were K-Nearest Neighbors Regressor, Quantile Regressor, and Radius Neighbors Regressor, which were also identified as suboptimal in the previous dataset context. For the selected best models, further analyses were conducted based on the error distribution related to MAE and MSE, and by using SHAP summary plots, correlation graphs, and Bland-Altman plots (Figure 4), with particular attention given to the Ridge and Theil-Sen Regressor models, which showed the most promising performance in terms of correctly classifying potentially symptomatic subjects. For the Ridge model, the most relevant variables identified with the SHAP summary plot (Figure 4a) were age, the estimated PWV value derived from the radial and tibial signals, and the carotid-femoral distance, all characteristics plausibly correlated with the physiological output. The corresponding correlation graph (Figure 4b) shows a good distribution of the data. The Bland-Altman analysis (Figure 4c) shows virtually no bias and a standard deviation supporting the reliability of the model. The second model, Theil-Sen Regressor, presents correlation (Figure 4e) and Bland-Altman (Figure 4f) analysis results comparable to those of Ridge, although with slightly higher bias and a marginally higher standard deviation. An interesting aspect revealed by the SHAP summary plot analysis (Figure 4d) is the strong dependence of the model on the information regarding radial and tibial PTT, as well as their differential, for estimating the output value. This feature makes Theil-Sen Regressor an ideal candidate for implementation in wearable devices, as its accuracy does not rely on auxiliary information but is solely based on data easily derived from the input signals. To further assess their generalization capability, the two models were evaluated through a LOO validation scheme, whereby each of the 90 subjects in the dataset was sequentially excluded from training and used as an independent test case. The Ridge Regressor model reported a mean absolute error of $-0.012\,\mathrm{m/s}$ and an associated standard deviation of $0.981\,\mathrm{m/s}$, while the Theil-Sen Regressor demonstrated slightly worst accuracy, yielding a mean error of $-0.103\,\mathrm{m/s}$ and a standard deviation of $1.037\,\mathrm{m/s}$. These findings, aligned with the clinical benchmarking criteria previously outlined, reinforce the robustness of both models, with the Ridge Regressor showing comparatively better overall performance.

IV. Discussion

A. Comparative analysis of acquisition configurations

To provide a comprehensive assessment of the predictive capabilities and practical implications of the proposed models, a comparative analysis between the two acquisition configurations, Carotid–Radial and Radial–Tibial, was conducted. In the Carotid–Radial configuration, the most accurate models, including Poisson and ARD Regressors, demonstrated consistent performance but relied strongly on variables such as age, carotid-femoral distance, and variability in radial PTT. This dependence on centrally derived or auxiliary parameters suggests a physiologically coherent model but potentially limits implementation in wearable or minimally supervised contexts. Conversely, models developed from the Radial–Tibial configuration—particularly Ridge and Theil–Sen Regressors—achieved comparable predictive accuracy with significantly reduced reliance on central anatomical references. These models prioritized locally obtainable features such as radial and tibial pulse transit times and their differential, in addition to subject age. This reduced dependency enhances suitability for integration in wearable systems, offering advantages in terms of acquisition simplicity, operator independence, and scalability. This perspective is reinforced by recent experimental developments demonstrating fully wireless, real-time PWV monitoring platforms [28], which confirm the feasibility of low-complexity integration for autonomous cardiovascular assessment. Overall, both configurations proved high accuracy for cf-PWV estimation. However, the Radial–Tibial setup emerges as more versatile and technically favorable for decentralized monitoring solutions, especially in ambulatory or consumer health applications.

B. Comparison to Related Works

The results highlight the significant potential of regression models in estimating cf-PWV, even using more peripheral signal acquisition sites, such as the radial or tibial regions. In both experimental configurations, Carotid-Radial and Radial-Tibial, the observed LOO errors fall within ranges consistent with current recommendations, supporting the reliability of the predictions generated by the developed models. This study contributes to an innovative research direction aimed at exploring the use of peripheral acquisition sites for PWV analysis to develop less invasive and more easily integrable solutions for wearable devices. Recent literature, such as the works presented in [29], [30], has reported promising

results using regression approaches similar to those adopted in this study, applied to photoplethysmographic (PPG) signals. However, these studies rely solely on synthetic data, which is inherently limited in validity due to the lack of confirmation on accurate data. In [31], an interesting analysis was conducted on PPG signals. However, it focused solely on the R^2 metric without providing a detailed evaluation of error distribution, a crucial aspect for the clinical validation of a model. The work presented in [27] provides an additional relevant contribution based on the analysis of PPG signals. It presents a methodology fully comparable to the one adopted in this study. The number of subjects involved and the quality of the results obtained are similar, further reinforcing the validity and robustness of the findings presented in this study. Using photoplethysmographic (PPG) signals opens up extremely promising scenarios in terms of wearability and ease of integration into wearable devices. However, this approach also presents particular challenges. Specifically, in the aforementioned literature, regression models are commonly trained not only using features of the subject but also morphological features directly extracted from the PPG signal. Such dependency introduces a significant constraint, as it ties the model's performance to the hardware and the sensors used during acquisition. The morphology of the signal can vary significantly depending on the sensor's position, the sensor itself, or the conditioning circuit employed, thus compromising the model's generalizability. In contrast, the approach proposed in this study is designed to be independent of the acquisition system used. The models developed are trained exclusively on features derived directly from the clinical gold standard for PWV, that is characterized by high reliability and reproducibility. This methodological choice allows the predictive process to be decoupled from the specific technicalities of the hardware used, making the model more robust and transferable to heterogeneous application contexts. An innovative aspect of this work is the use of the tibial site for signal acquisition, an anatomical area that has yet to be systematically explored in current scientific literature. Furthermore, recent advancements in flexible pressure sensors have opened new avenues for the design of compact, conformable, and biocompatible acquisition systems, which could further enhance the wearability and integration of PWV monitoring platforms [32].

C. Limitation and Future Works

The population included in this study was selected in accordance with the clinical reference parameters recommended in the field. Moreover, the acquisition protocol was designed to minimize the effects of inter-operator variability and potential external factors, thereby ensuring greater reliability in the measurements. This study has demonstrated the feasibility of using peripheral sites for pulse wave acquisition in order to estimate, with high accuracy, cf-PWV. However, the development of a robust and clinically applicable model requires extending the training phase to a significantly larger cohort, including both healthy and pathological subjects, as well as individuals from diverse backgrounds. This is essential to ensure that the training population adequately reflects the heterogeneity of modern society, thereby enhancing the model's generalizability and real-world applicability. The expansion of the dataset would enable the adoption of more advanced modeling techniques, such as the use of neural networks. It should also be noted that the data set used in the present study includes only data from healthy individuals, which limits the generalizability of the results. Moreover, as highlighted in recent studies [33], cf-PWV values differ significantly across populations, even under equivalent cardiovascular conditions. Notably, a substantial variation in cf-PWV has also been observed between gender [34], although no clear correlation has been established between these differences and atherosclerotic risk. A natural progression of this work could involve integrating data from individuals with cardiovascular diseases and different populations, in order to assess the model's ability to generalize effectively to clinically heterogeneous populations.

V. Conclusion

PWV in clinical settings is gaining increasing importance providing reliable prognostic information on the health status of the cardiovascular system. However, the traditional anatomical sites used for PWV estimation, such as the carotid and femoral sites, are not always easy to identify and often require a high level of expertise from the healthcare provider. This study aims to train regression models capable of estimating cf-PWV from signals acquired at peripheral sites, such as the Carotid-Radial and Radial-Tibial pairs, using the gold standard system for this application, SphygmoCor, as the reference. The high reproducibility and accuracy of SphygmoCor have been transferred into the data used for training the predictive models, providing a high-quality input dataset. The models developed for both configurations demonstrated acceptable error values, although the sample size does not allow for a full validation in accordance with the recommendations for the development of new medical devices. An initial comparison indicates that the majority of Radial-Tibial models exhibit performance levels comparable to the Carotid–Radial ones, implying that the inclusion of the carotid site may not be essential for achieving accurate predictions. Similarly, the models trained on the Radial-Tibial data demonstrated comparable predictive performance. These findings open up promising application prospects, suggesting the potential to integrate these new acquisition sites into commercial devices, particularly in contexts where preferred sites are complex or impractical. This would contribute to fostering the adoption of PWV as a reference clinical indicator, even in non-cardiological healthcare settings, significantly expanding its dissemination and utility in daily clinical practice.

References

[1] H.-L. Kim and S.-H. Kim, "Pulse wave velocity in atherosclerosis," *Frontiers in cardiovascular medicine*, vol. 6, p. 41, 2019.

[2] A. Timmis, D. Kazakiewicz, N. Townsend, R. Huculeci, V. Aboyans, and P. Vardas, "Global epidemiology of acute coronary syndromes," *Nature Reviews Cardiology*, pp. 1–11, 2023.

[3] D. Kingsmore, B. Edgar, M. Rostron, C. Delles, and A. Brady, "A novel index for measuring the impact of devices on hypertension," *Scientific Reports*, vol. 13, no. 1, p. 13651, 2023.

[4] M. E. Safar, B. I. Levy, and H. Struijker-Boudier, "Current Perspectives on Arterial Stiffness and Pulse Pressure in Hypertension and Cardiovascular Diseases," *Circulation*, vol. 107, no. 22, pp. 2864–2869, 2003.

[5] R. A. Payne, I. B. Wilkinson, and D. J. Webb, "Arterial Stiffness and Hypertension: Emerging Concepts," *Hypertension*, vol. 55, no. 1, pp. 9–14, 2010.

[6] J. A. Chirinos, P. Segers, T. Hughes, and R. Townsend, "Large-Artery Stiffness in Health and Disease: JACC State-of-the-Art Review," *Journal of the American College of Cardiology*, vol. 74, no. 9, pp. 1237–1263, 2019.

[7] B. Aimagambetova, T. Ariko, S. Merritt, and T. Rundek, "Arterial stiffness measured by pulse wave velocity correlated with cognitive decline in hypertensive individuals: a systematic review," *BMC neurology*, vol. 24, no. 1, p. 393, 2024.

[8] N. Pilz, V. Heinz, T. Ax, L. Fesseler, A. Patzak, and T. L. Bothe, "Pulse wave velocity: methodology, clinical applications, and interplay with heart rate variability," *Reviews in Cardiovascular Medicine*, vol. 25, no. 7, p. 266, 2024.

[9] K. Sutton-Tyrrell, S. S. Najjar, R. M. Boudreau, L. Venkitachalam, V. Kupelian, E. M. Simonsick, R. Havlik, E. G. Lakatta, H. Spurgeon, S. Kritchevsky *et al.*, "Elevated Aortic Pulse Wave Velocity, a Marker of Arterial Stiffness, Predicts Cardiovascular Events in Well-Functioning Older Adults," *Circulation*, vol. 111, no. 25, pp. 3384–3390, 2005.

[10] L. M. Van Bortel, S. Laurent, P. Boutouyrie, P. Chowienczyk, J. Cruickshank, T. De Backer, J. Filipovsky, S. Huybrechts, F. U. Mattace-Raso, A. D. Protogerou *et al.*, "Expert consensus document on the measurement of aortic stiffness in daily practice using carotid-femoral pulse wave velocity," *Journal of hypertension*, vol. 30, no. 3, pp. 445–448, 2012.

[11] L. Xu, S. Zhou, L. Wang, Y. Yao, L. Hao, L. Qi, Y. Yao, H. Han, R. Mukkamala, and S. E. Greenwald, "Improving the accuracy and robustness of carotid-femoral pulse wave velocity measurement using a simplified tube-load model," *Scientific reports*, vol. 12, no. 1, p. 5147, 2022.

[12] A. Valerio, I. Buraioli, A. Sanginario, G. Mingrone, D. Leone, A. Milan, and D. Demarchi, "A region-based cross-correlation approach for tonometric carotid–femoral pulse wave velocity assessment," *Biomedical Signal Processing and Control*, vol. 93, p. 106161, 2024.

[13] A. Milan, G. Zocaro, D. Leone, F. Tosello, I. Buraioli, D. Schiavone, and F. Veglio, "Current assessment of pulse wave velocity: comprehensive review of validation studies," *Journal of hypertension*, vol. 37, no. 8, pp. 1547–1557, 2019.

[14] M. Butlin and A. Qasem, "Large Artery Stiffness Assessment Using SphygmoCor Technology," *Pulse*, vol. 4, no. 4, pp. 180–192, 2017.

[15] V. Fabian, L. Matera, K. Bayerova, J. Havlik, V. Kremen, J. Pudil, P. Sajgalik, and D. Zemanek, "Noninvasive assessment of aortic pulse wave velocity by the brachial occlusion-cuff technique: comparative study," *Sensors*, vol. 19, no. 16, p. 3467, 2019.

[16] T. Shoji, A. Nakagomi, S. Okada, Y. Ohno, and Y. Kobayashi, "Invasive validation of a novel brachial cuff-based oscillometric device (SphygmoCor XCEL) for measuring central blood pressure," *Journal of hypertension*, vol. 35, no. 1, pp. 69–75, 2017.

[17] M. Hwang, J. Yoo, H. Kim, C. Hwang, K. Mackay, O. Hemstreet, W. Nichols, and D. Christou, "Validity and reliability of aortic pulse wave velocity and augmentation index determined by the new cuff-based SphygmoCor Xcel," *Journal of human hypertension*, vol. 28, no. 8, pp. 475–481, 2014.

[18] P. Salvi, G. Lio, C. Labat, E. Ricci, B. Pannier, and A. Benetos, "Validation of a new non-invasive portable tonometer for determining arterial pressure wave and pulse wave velocity: the PulsePen device," *Journal of hypertension*, vol. 22, no. 12, pp. 2285–2293, 2004.

[19] I. Buraioli, D. Lena, A. Sanginario, D. Leone, G. Mingrone, A. Milan, and D. Demarchi, "A New Noninvasive System for Clinical Pulse Wave Velocity Assessment: The Athos Device," *IEEE Transactions on Biomedical Circuits and Systems*, vol. 15, no. 1, pp. 133–142, 2021.

[20] D. Leone, I. Buraioli, G. Mingrone, D. Lena, A. Sanginario, F. Vallelonga, F. Tosello, E. Avenatti, M. Cesareo, A. Astarita *et al.*, "Accuracy of a new instrument for noninvasive evaluation of pulse wave velocity: the arterial stiffness faithful tool assessment project," *Journal of Hypertension*, vol. 39, no. 11, pp. 2164–2172, 2021.

[21] S. S. Hickson, M. Butlin, J. Broad, A. P. Avolio, I. B. Wilkinson, and C. M. McEniery, "Validity and repeatability of the Vicorder apparatus: a comparison with the SphygmoCor device," *Hypertension research*, vol. 32, no. 12, pp. 1079–1085, 2009.

[22] M. Ring, M. J. Eriksson, J. R. Zierath, and K. Caidahl, "Arterial stiffness estimation in healthy subjects: a validation of oscillometric (Arteriograph) and tonometric (SphygmoCor) techniques," *Hypertension Research*, vol. 37, no. 11, pp. 999–1007, 2014.

[23] R. Asmar, J. Topouchian, B. Pannier, A. Benetos, M. Safar *et al.*, "Pulse wave velocity as endpoint in large-scale intervention trial. The Complior® study," *Journal of hypertension*, vol. 19, no. 4, pp. 813–818, 2001.

[24] T. Sondej, I. Jannasz, K. Sieczkowski, A. Dobrowolski, K. Obiała, T. Targowski, and R. Olszewski, "Validation of a new device for photoplethysmographic measurement of multi-site arterial pulse wave velocity," *biocybernetics and biomedical engineering*, vol. 41, no. 4, pp. 1664–1684, 2021.

[25] R. A. Rodriguez, V. Cronin, T. Ramsay, D. Zimmerman, M. Ruzicka, and K. D. Burns, "Reproducibility of carotid-femoral pulse wave velocity in end-stage renal disease patients: methodological considerations," *Canadian Journal of Kidney Health and Disease*, vol. 3, p. 109, 2016.

[26] B. Spronck, D. Terentes-Printzios, A. P. Avolio, P. Boutouyrie, A. Guala, A. Jerončić, S. Laurent, E. C. Barbosa, J. Baulmann, C.-H. Chen *et al.*, "2024 recommendations for validation of noninvasive arterial pulse wave velocity measurement devices," *Hypertension*, vol. 81, no. 1, pp. 183–192, 2024.

[27] A. Gentilin, C. Tarperi, A. Cevese, A. V. Mattioli, and F. Schena, "Estimation of carotid-femoral pulse wave velocity from finger photoplethysmography signal," *Physiological Measurement*, vol. 43, no. 7, p. 075011, 2022.

[28] A. Valerio, I. Buraioli, A. Sanginario, D. Leone, G. Mingrone, A. Milan, and D. Demarchi, "A new true wireless system for real-time pulse wave velocity assessment," *IEEE Sensors Journal*, vol. 24, no. 15, pp. 24 365–24 376, 2024.

[29] V. Debuchy, M. Khalifa, P. Tresson, N. Thirion-Moreau, and E. Moreau, "Machine learning techniques applied to in-silico pulse wave velocity estimation based on photoplethysmographic signals," in *2024 32nd European Signal Processing Conference (EUSIPCO)*. IEEE, 2024, pp. 1716–1720.

[30] M. A. Bahloul, A. Chahid, and T.-M. Laleg-Kirati, "A multilayer perceptron-based carotid-to-femoral pulse wave velocity estimation using ppg signal," in *2021 IEEE EMBS International Conference on Biomedical and Health Informatics (BHI)*. IEEE, 2021, pp. 1–6.

[31] J. M. V. Garcia, M. A. Bahloul, and T.-M. Laleg-Kirati, "A multiple linear regression model for carotid-to-femoral pulse wave velocity estimation based on schrodinger spectrum characterization," in *2022 44th Annual International Conference of the IEEE Engineering in Medicine & Biology Society (EMBC)*. IEEE, 2022, pp. 143–147.

[32] A. Sanginario, I. Buraioli, M. Boscherini, S. Vitale, C. Sabrina, D. Botto, D. Leone, A. Milan, A. Ciesielski, P. Samorì, and D. Demarchi, "Reduced graphene oxide-based flexible pressure sensor for biomedical applications," *IEEE Sensors Journal*, vol. 24, no. 22, pp. 37 090–37 103, 2024.

[33] K. M. van der Sluijs, J. Thannhauser, I. M. Visser, P. Nabeel, K. V. Raj, A. E. Malik, K. D. Reesink, T. M. Eijsvogels, E. A. Bakker, P. Kaur *et al.*, "Central and local arterial stiffness in white europeans compared to age-, sex-, and bmi-matched south asians," *PloS one*, vol. 18, no. 8, p. e0290118, 2023.

[34] I. Jannasz, T. Sondej, T. Targowski, M. Mańczak, K. Obiała, A. P. Dobrowolski, and R. Olszewski, "Relationship between the central and regional pulse wave velocity in the assessment of arterial stiffness depending on gender in the geriatric population," *Sensors*, vol. 23, no. 13, p. 5823, 2023.